Electronic Supplementary Material (ESI) for Dalton Transactions.

Supporting Information

Synthesis, Structural Characterisation, and Cytotoxicity Studies of Bi, W, and Mo containing Homo- and Hetero-bimetallic Polyoxometalates

Content:

Experimental Details

Energy Dispersive X-ray Spectroscopy

EDX spectrum of the white solid which precipitated from the reaction of $[(NH_4)_6Mo_7O_{24}]\cdot 4H_2O$, 2,5-dimethylsulfonic acid and $Bi(NO_3)_3\cdot 5H_2O$ and EDX for compounds **1**, **2** and **3**

Crystallography Details

PXRD Study

PXRD patterns of bulk crystalline sample of compound **1**, **2** and **3**

Summary of crystallographic data for **1**, **2** and **3**

ESI-MS Studies

ESI-MS of compound **1** and predicted isotope patterns

Raman Spectroscopy

Raman Spectra of compound **1**, **2** and **3**

Thermogravimetric Analysis (TGA)

TGA plots of compound **1**, **2** and **3**

Experimental

General Considerations

All chemicals were purchased from Sigma Aldrich or Alfa Aesar Chemical Co and used as received, unless otherwise stated. Raman Infrared spectra were recorded on a WITec 300R Raman microscope with 532 nm excitation 5x3 sec acquisitions averaged; 3 mW at sample, Objective 50X. IR frequencies are reported in wavenumbers with the relative intensities indicated as strong (s), medium (m) or weak (w). Elemental microanalyses were performed at Monash University using a 2400 Series II CHNS/O Elemental Analyser. Thermogravimetric analysis (TGA) was carried out using a Mettler Toledo TGA/DSC 1 Star System, 10 degrees/min, N2 flow rate of 30ml/min. Mass spectrometry (ESI) was performed on a Micromass Platform QMS spectrometer with an electrospray source and a cone voltage of 35 eV, or performed on an Agilent 6220 Accurate Mass LC-TOF system with the Agilent Mutlimode Source and a capillary voltage of 3500 V. All samples were analysed in water. Agilent MassHunter Qualitative Analysis B.06.00 was used to analyse the spectra and Isotope Distribution Calculator was used to predict specific isotope patterns.

Samples analysed by scanning electron microscopy (SEM) and energy dispersive X-ray spectroscopy (EDX) were mounted, using carbon adhesive discs, onto an SEM specimen stub and carbon coated. Analyses were carried out on a JEOL JSM-7001F FEGSEM with an Oxford Instruments AZtec X-ray analysis system. Samples were studied using a 15 kV accelerating voltage and the data was processed using Oxford AZtec software.

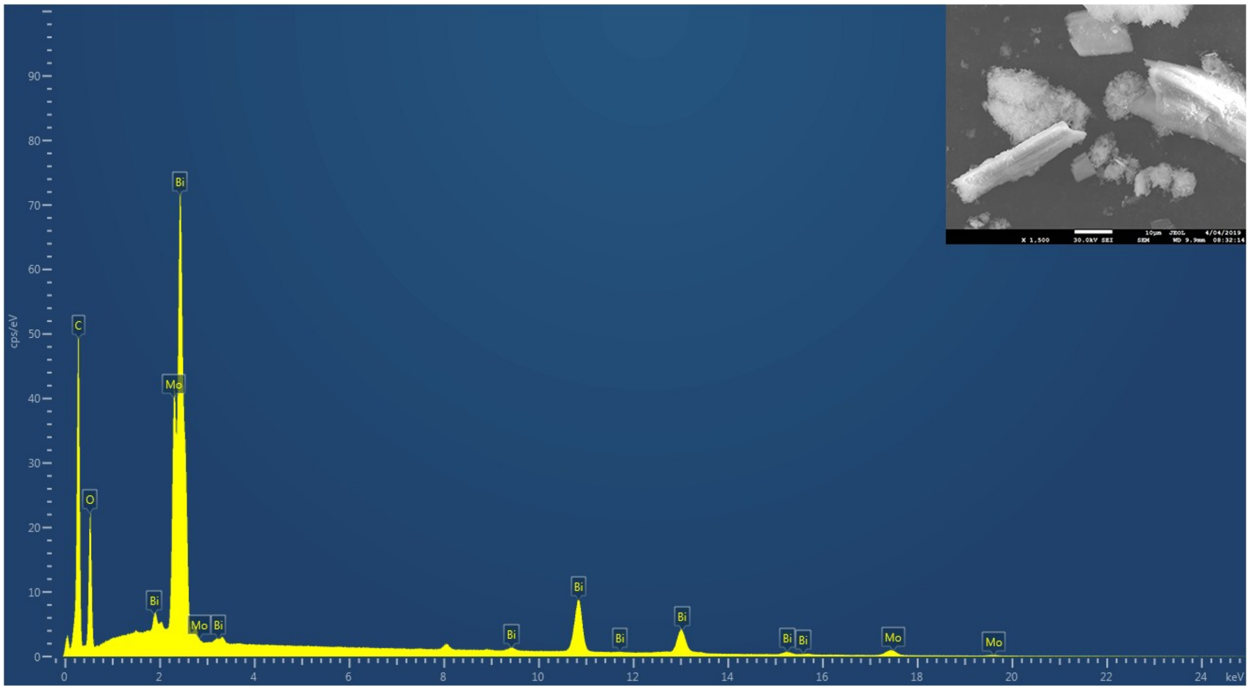

Figure S1: Representative EDX spectrum of the white solid which precipitated from the reaction of $[(NH_4)_6Mo_7O_{24}]\cdot 4H_2O$, 2,5-dimethylsulfonic acid and $Bi(NO_3)_3\cdot 5H_2O$. EDX spectrum collected on the SEM at 30 kV from the region showed in the inset. The solid was heterogenous however Bi and Mo was present in all spectra. Note: The signal seen for carbon in Figure S1 is from the sample coating.

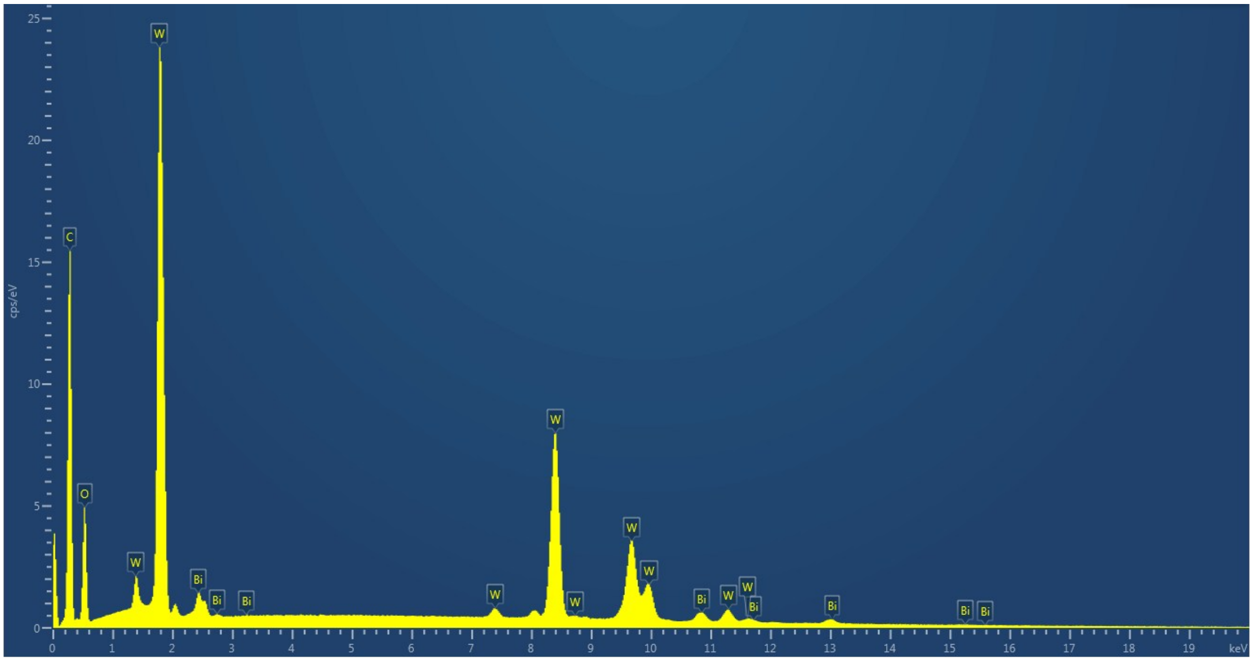

Figure S2: EDX spectrum of compound $(NH_4)_{14}[Bi_2W_{22}O_{76}]\cdot 14H_2O$ (**1**$\cdot 14H_2O$), showing the presence of Bi and W.

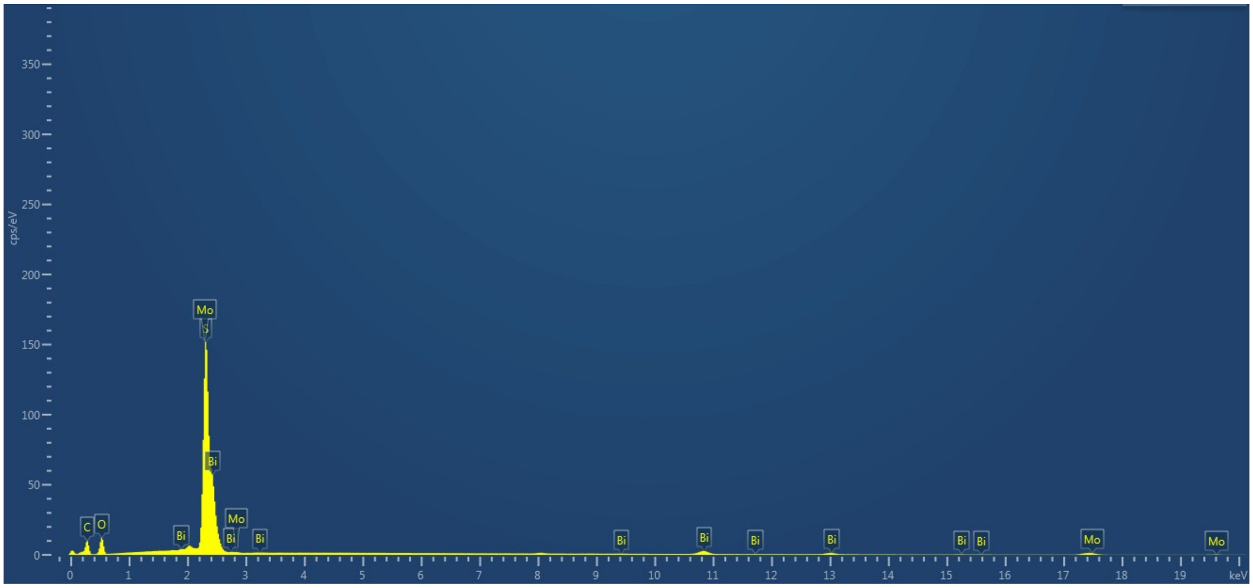

Figure S3: EDX spectrum of compound $(NH_4)[Bi(DMSO)_7][Mo_8O_{26}]\cdot H_2O$ (**2**$\cdot H_2O$)**,** showing the presence of Bi and Mo.

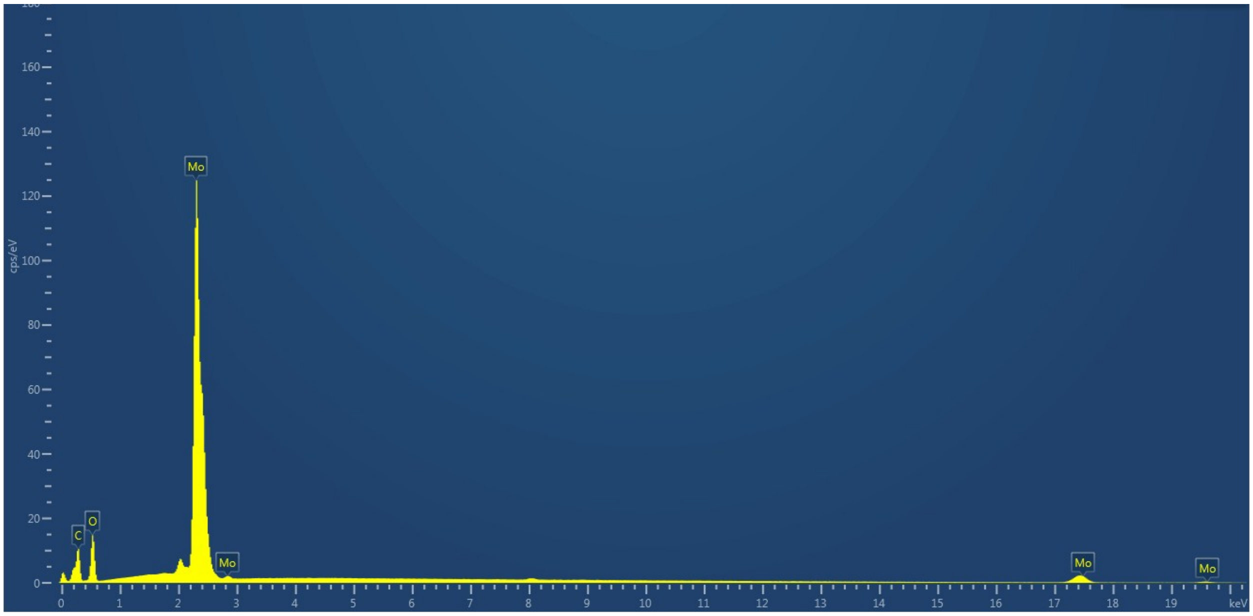

Figure S4: EDX spectrum of compound $[(NH_4)_4(Mo_{36}O_{108}(OH)_4\cdot16H_2O)]\cdot45H_2O$ (**3**$\cdot45H_2O$)**,** showing the presence of Mo.

PXRD Study

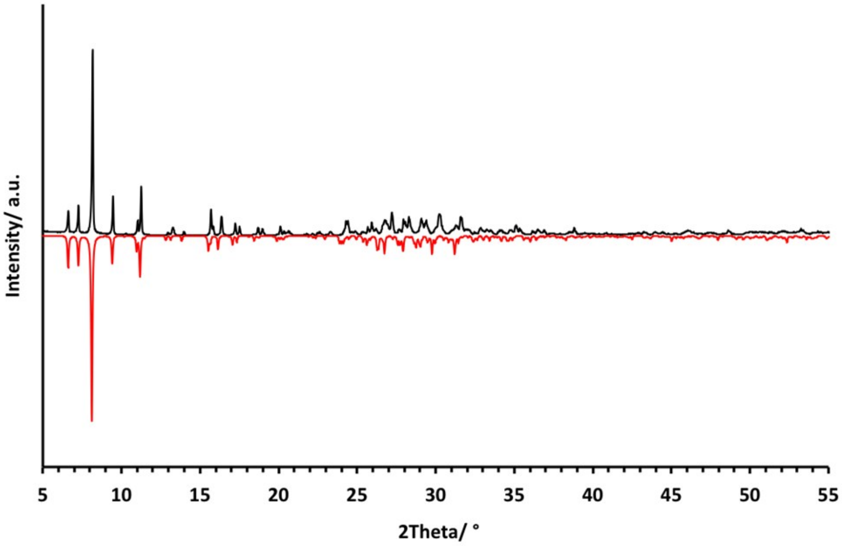

Figure S5: PXRD pattern of bulk crystalline product of compound $(NH_4)_{14}[Bi_2W_{22}O_{76}]\cdot 14H_2O$ (**1**$\cdot 14H_2O$) (black) and the calculated PXRD pattern (red) obtained from the single crystal X-ray diffraction studies.

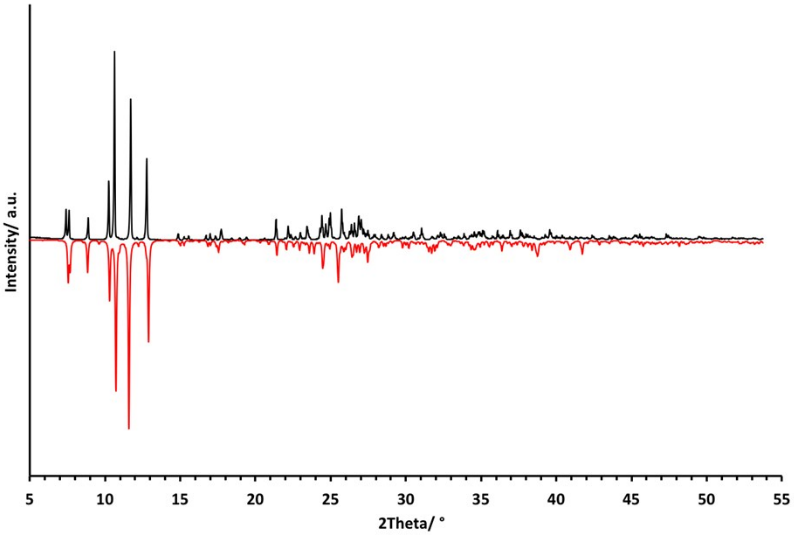

Figure S6: PXRD pattern of bulk crystalline product of compound $(NH_4)[Bi(DMSO)_7][Mo_8O_{26}]\cdot H_2O$ (**2**$\cdot H_2O$) (black) and the calculated PXRD pattern (red) obtained from the single crystal X-ray diffraction studies.

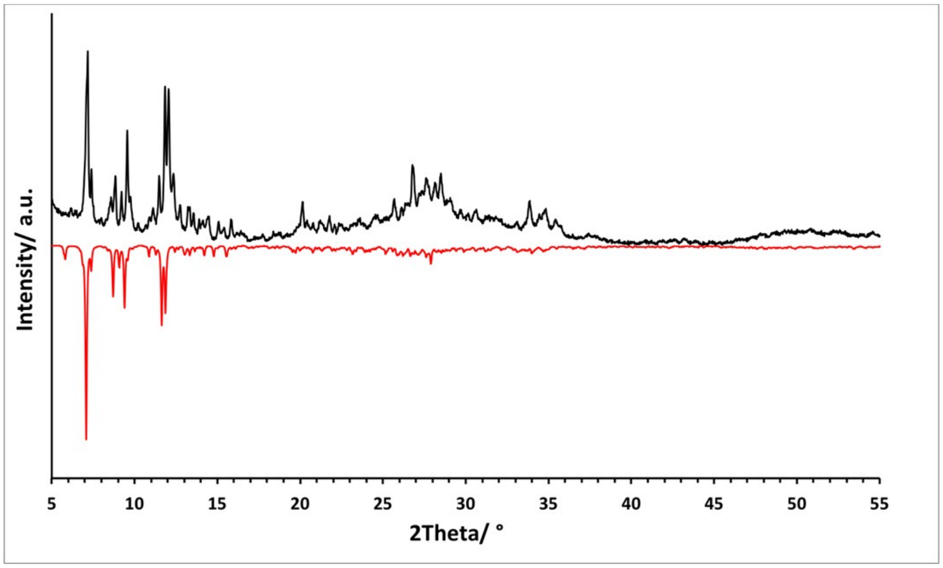

Figure S7: PXRD pattern of bulk crystalline product of compound $[(NH_4)_4(Mo_{36}O_{108}(OH)_4{\cdot}16H_2O)]{\cdot}45H_2O$ (**3**$\cdot 45H_2O$) (black) and the calculated PXRD pattern (red) obtained from the single crystal X-ray diffraction studies.

Crystallography Details

Crystallographic data for compounds $(NH_4)_{14}[Bi_2W_{22}O_{76}]{\cdot}14H_2O$ (**1**$\cdot 14H_2O$), $(NH_4)[Bi(DMSO)_7][Mo_8O_{26}]{\cdot}H_2O$ (**2**$\cdot H_2O$) and $[(NH_4)_4(Mo_{36}O_{108}(OH)_4{\cdot}16H_2O)]{\cdot}45H_2O$ (**3**$\cdot 45H_2O$) was obtained on a Bruker X8 APEXII CCD diffractometer equipped with an OXFORD Cryosystems 700 Cryostream and cooled to 123(2) K. Data was collected with monochromatic (graphite) MoK_α radiation (λ = 0.71073 Å) and processed using the Bruker Apex2 v2012.2.0 software; Lorentz, polarization and multi-scan – SADABS[1] were applied. The structures were solved by direct method using the ShelXS-97[3] and refined by full-matrix least-squares procedure using ShelLX-97.[4] Non-hydrogen atoms were refined with anisotropic thermal parameters. Hydrogen atoms attached to C were placed in calculated positions using a riding model with C-H distances of 0.99 Å and $U_{iso}(H) = 1.2{\times}U_{eq}(C)$. All data for compounds **1**, **2** and **3** has been deposited with the Cambridge Crystallographic Database with CCDC numbers 1916373-1916375.

Table S1: Crystallographic data and structure refinement for compounds **1**, **2** and **3**.

	Compound **1**	Compound **2**	Compound **3**	Compound **3’**
Formula	$Bi_2N_{14}O_{88}W_{22}H_{80}$	$C_{16}H_{54}BiMo_8NO_{35}S_8$	$H_{182}Mo_{36}N_4O_{177}$	$H_{84}Mo_{36}N_4O_{142}$
M_r	6147.11	2053.73	6225.20	5866.45
Crystal size [mm]	0.23 x 0.20 x 0.17	0.32 x 0.21 x 0.17	0.31 x 0.24 x 0.18	0.28 x 0.20 x 0.16
Crystal system	Monoclinic	Monoclinic	Monoclinic	Triclinic
Space group	C2/m	$P2_1/c$	C2/c	P-1
a [Å]	17.4754(17)	11.6976(7)	39.510(2)	13.8050(16)
b [Å]	18.5453(15)	23.1883(13)	19.6993(10)	15.6017(19)
c [Å]	14.5934(14)	20.2723(11)	25.1554(13)	16.541(2)
α [°]	90°	90°	90°	79.724(6)°
β [°]	114.501(5)	102.973(3)	124.448(2)	79.189(6)°
γ [°]	90°	90°	90°	67.936(5)°
V [$Å^3$]	4303.6(7)	5358.5(5)	16145.6(15)	3220.3(7)
Z	2	4	4	1
T [K]	173(2)	173(2)	173(2)	173(2)
ρcalcd. [mg m^{-3}]	4.713	2.541	2.584	2.983
μ [mm^{-1}]	33.462	5.481	2.817	3.500
Reflections collected/unique	12205	65486	84630	25994
Rint	0.0376	0.0768	0.0460	0.1444
$R1$ [$I > 2\sigma(I)$]	0.0438	0.0363	0.0592	0.0775
$wR2$ (all data)	0.1012	0.0659	0.1435	0.2659
GoF	1.064	1.026	1.094	1.077

ESI-MS Studies

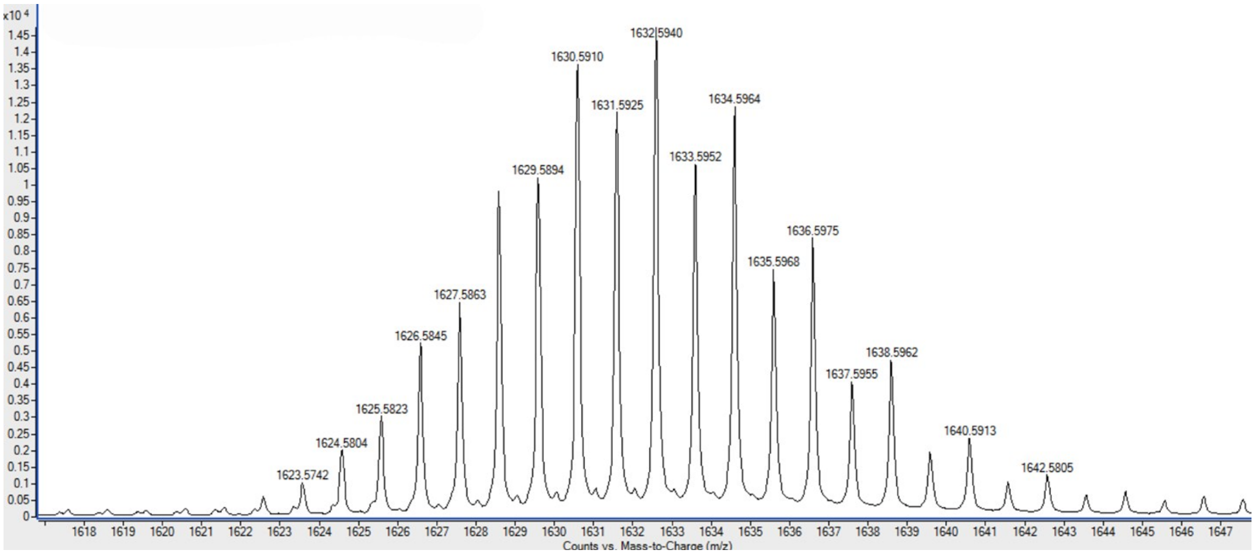

Figure S8: Section of the ESI-MS of compound $(NH_4)_{14}[Bi_2W_{22}O_{76}]\cdot14H_2O$ (**1**$\cdot14H_2O$) (sample run in water, within 20 minutes of preparation). Signal at m/z 1632.59identified as $[BiW_6O_{20}]^-$.

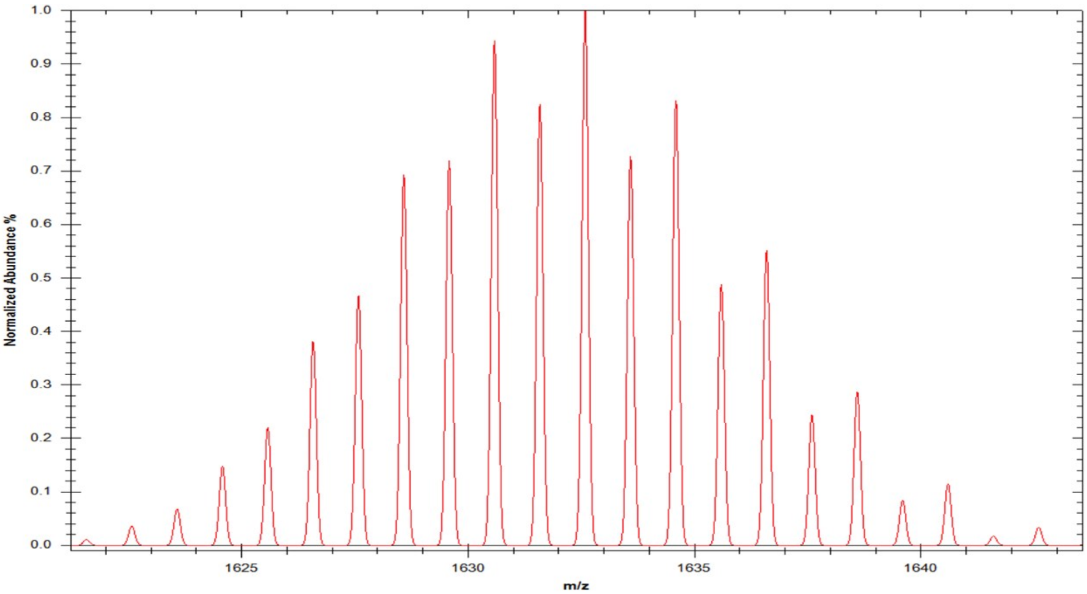

Figure S9: Predicted ESI-MS isotope pattern for $[BiW_6O_{20}]^-$ using Agilent MassHunter software.

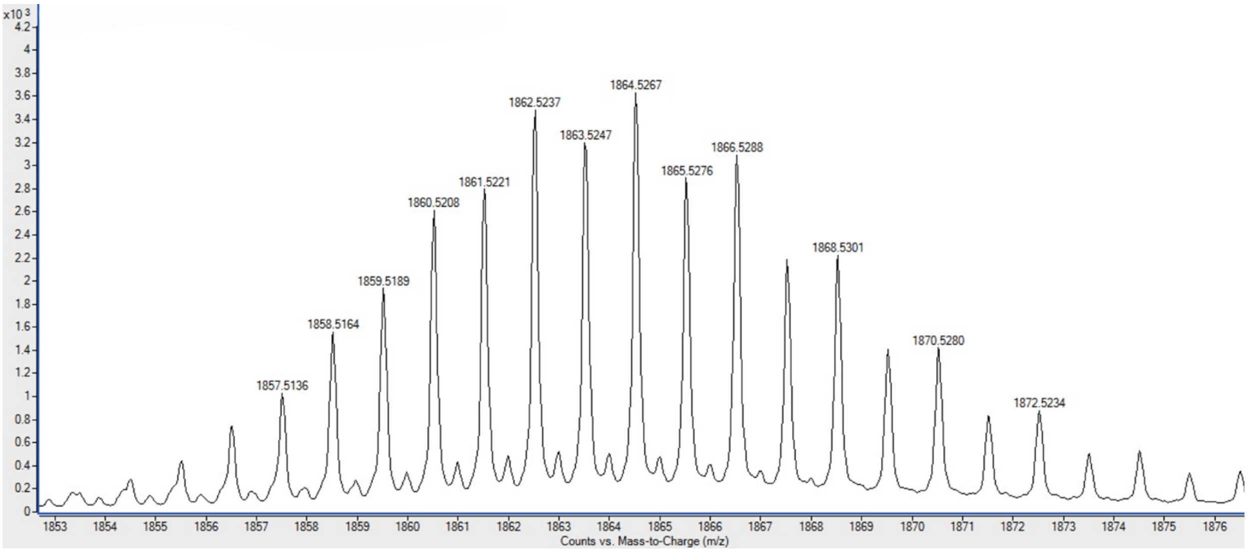

Figure S10: Section of the ESI-MS of compound $(NH_4)_{14}[Bi_2W_{22}O_{76}]\cdot 14H_2O$ (**1**$\cdot 14H_2O$) (sample run in water, within 20 minutes of preparation). Signal at m/z 1864.52 identified as $[BiW_7O_{23}]^-$.

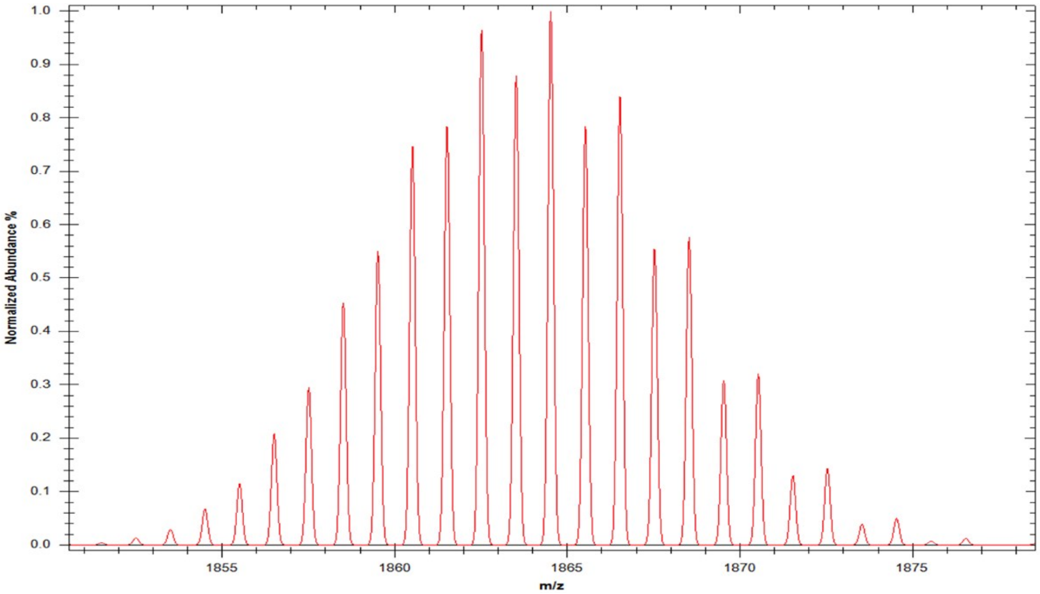

Figure S11: Predicted ESI-MS isotope pattern for $[BiW_7O_{23}]^-$ using Agilent MassHunter software.

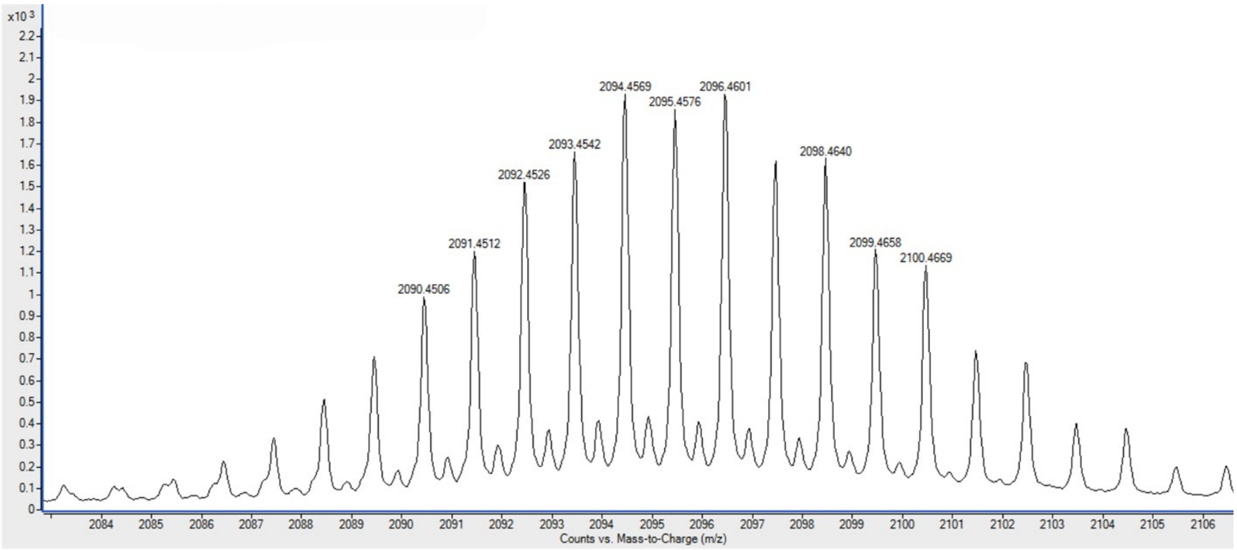

Figure S12: Section of the ESI-MS of compound $(NH_4)_{14}[Bi_2W_{22}O_{76}]\cdot 14H_2O$ (**1**$\cdot 14H_2O$) (sample run in water, within 20 minutes of preparation). Signal at m/z 2094 identified as $[BiW_8O_{26}]^-$.

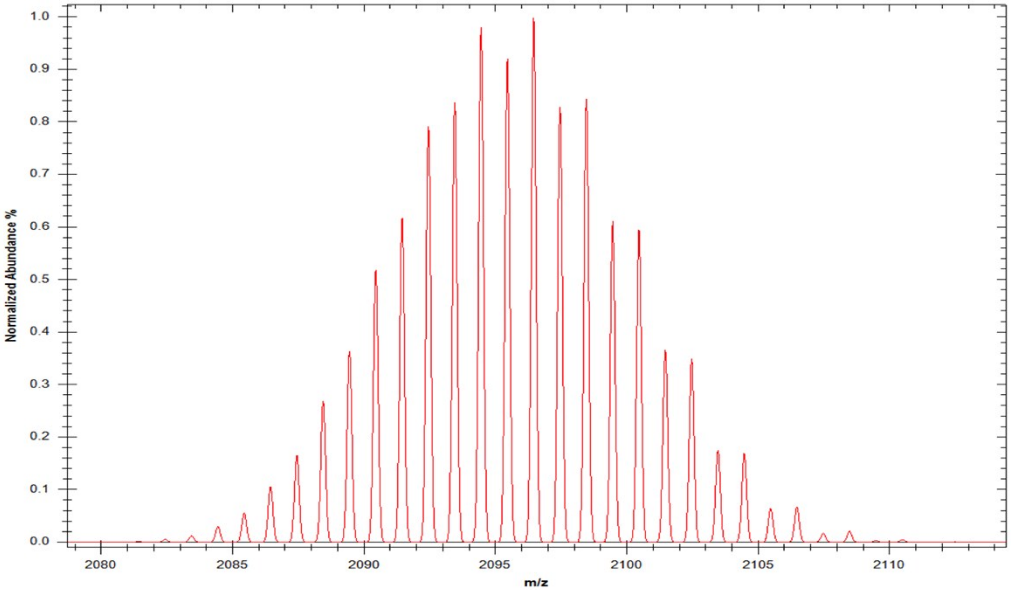

Figure S13: Predicted ESI-MS isotope pattern $[BiW_8O_{26}]^-$ using Agilent MassHunter software.

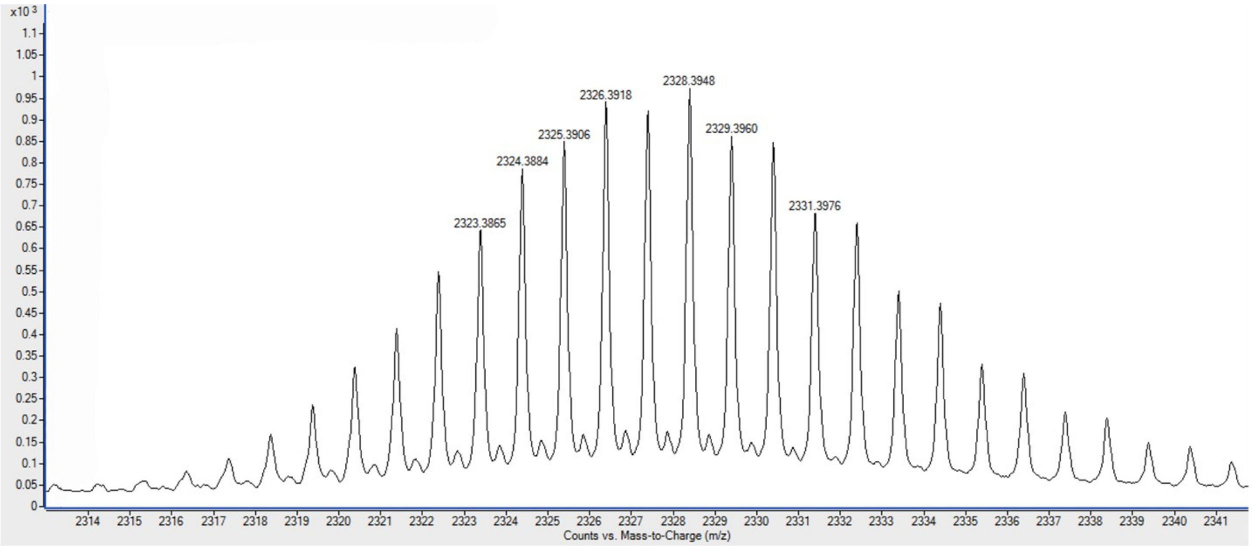

Figure S14: Section of the ESI-MS of compound $(NH_4)_{14}[Bi_2W_{22}O_{76}]\cdot 14H_2O$ (**1**$\cdot 14H_2O$) (sample run in water, within 20 minutes of preparation). Signal at m/z 2328.39 identified as $[BiW_9O_{29}]^-$.

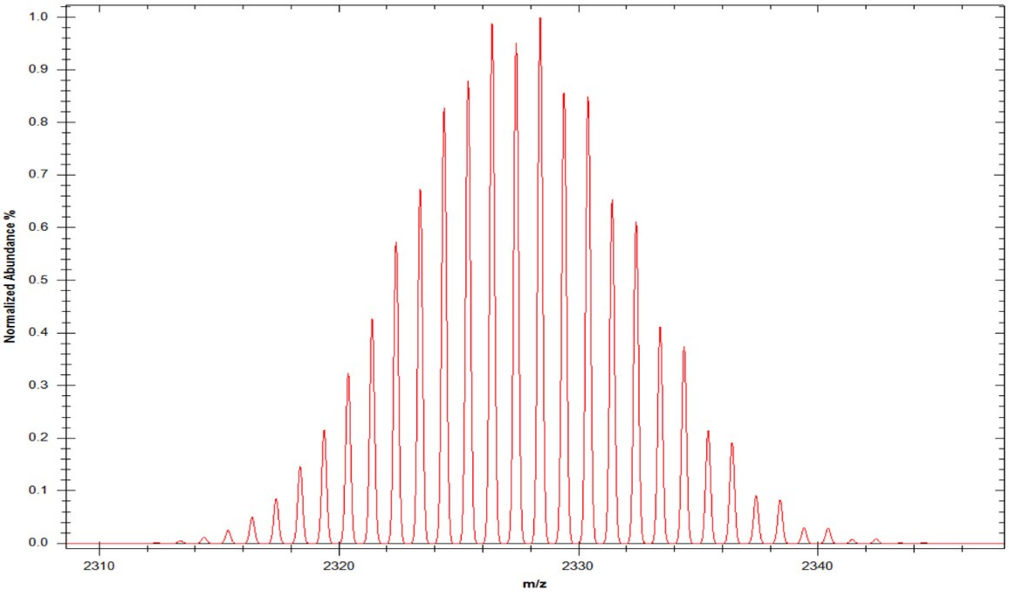

Figure S15: Predicted ESI-MS isotope pattern for $[BiW_9O_{29}]^-$ using Agilent MassHunter software.

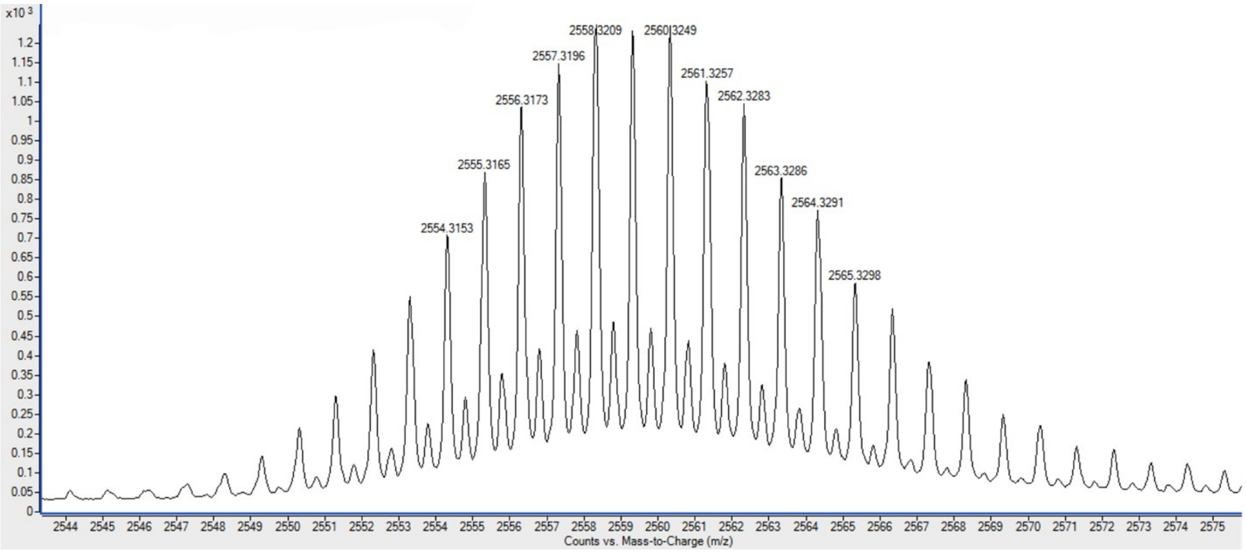

Figure S16: Section of the ESI-MS of compound $(NH_4)_{14}[Bi_2W_{22}O_{76}]\cdot 14H_2O$ (**1**$\cdot 14H_2O$) (sample run in water, within 20 minutes of preparation). Signal at m/z 2558.32 identified as $[BiW_{10}O_{32}]^-$.

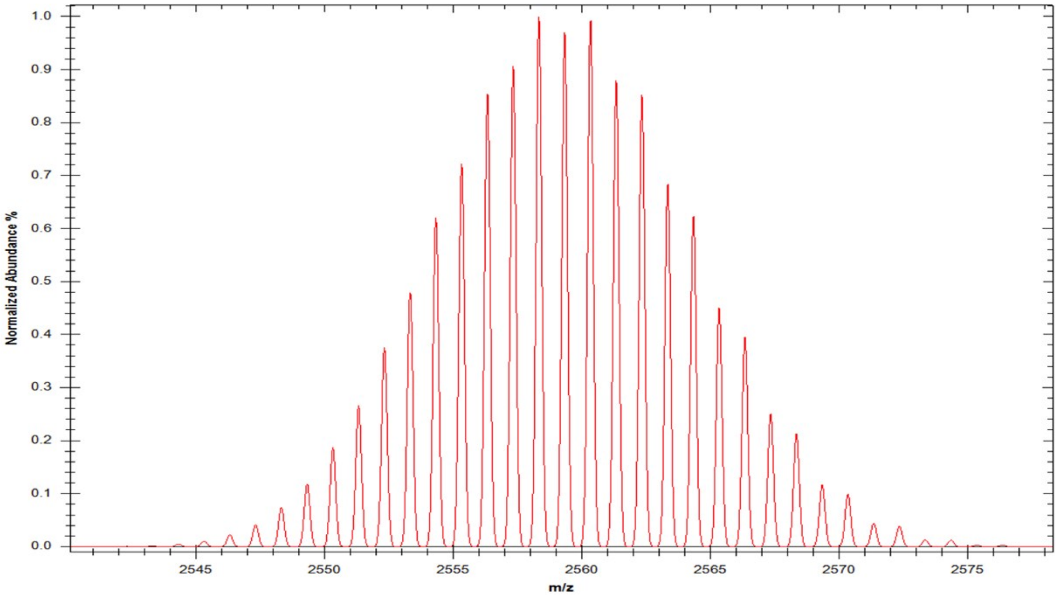

Figure S17: Predicted ESI-MS isotope pattern for $[BiW_{10}O_{32}]^-$ using Agilent MassHunter software.

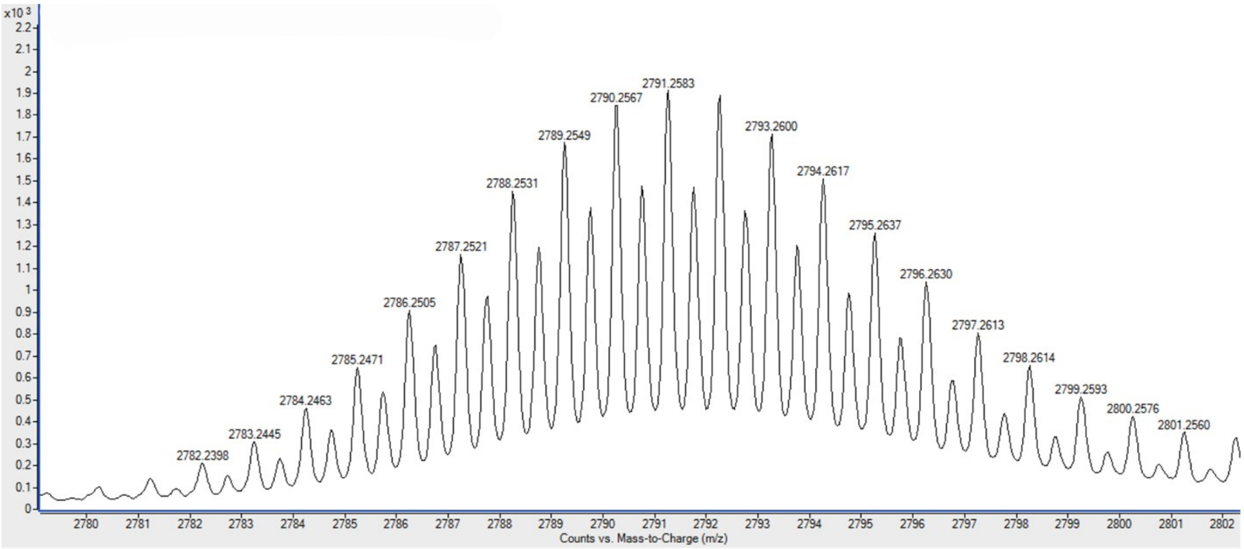

Figure S18: Section of the the ESI-MS of compound $(NH_4)_{14}[Bi_2W_{22}O_{76}]\cdot14H_2O$ (**1**$\cdot14H_2O$) (sample run in water, within 20 minutes of preparation). Signal at m/z 2791.25 identified as $[BiW_{11}O_{35}]^-$.

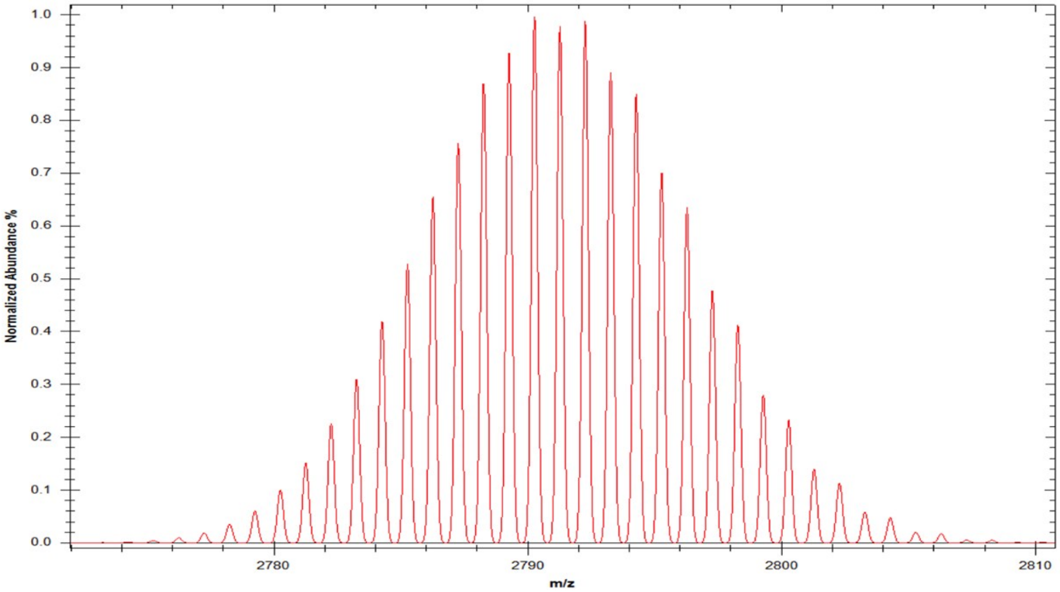

Figure S19: Predicted ESI-MS isotope pattern for $[BiW_{11}O_{35}]^-$ using Agilent MassHunter software.

Raman Spectroscopy

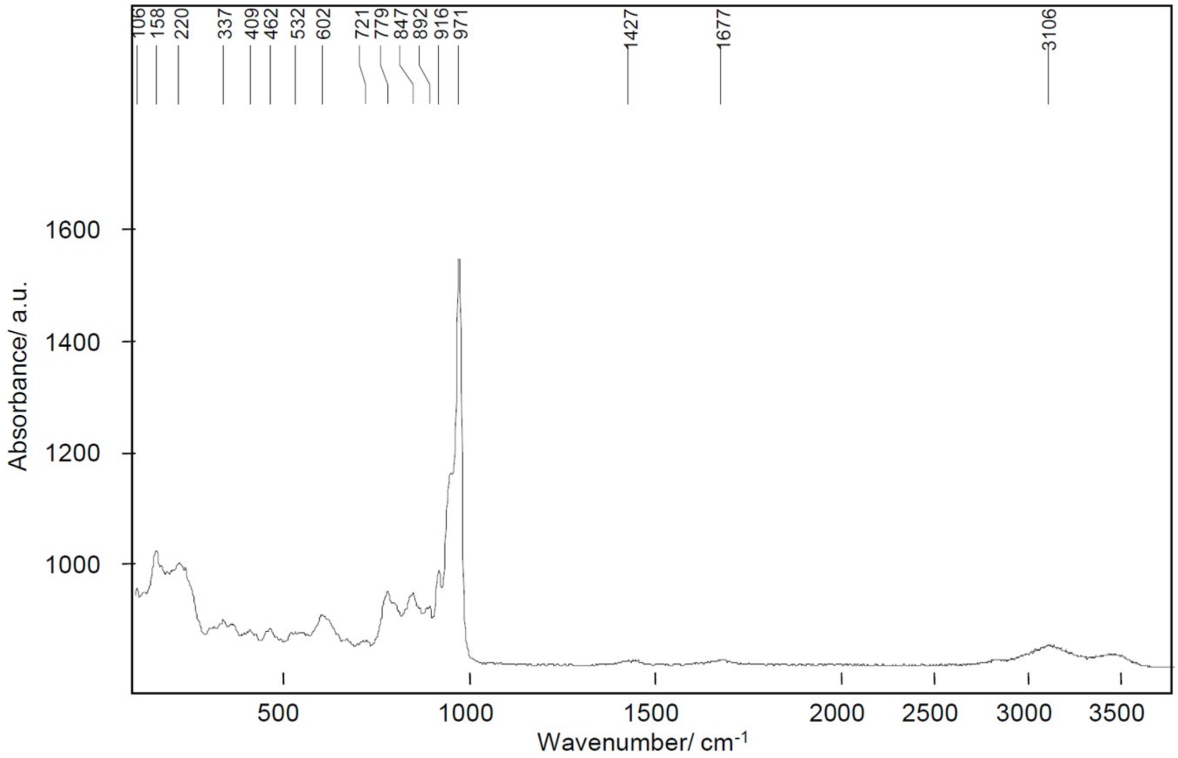

Figure S20: Raman spectrum of compound $(NH_4)_{14}[Bi_2W_{22}O_{76}]\cdot 14H_2O$ (**1**$\cdot 14H_2O$)

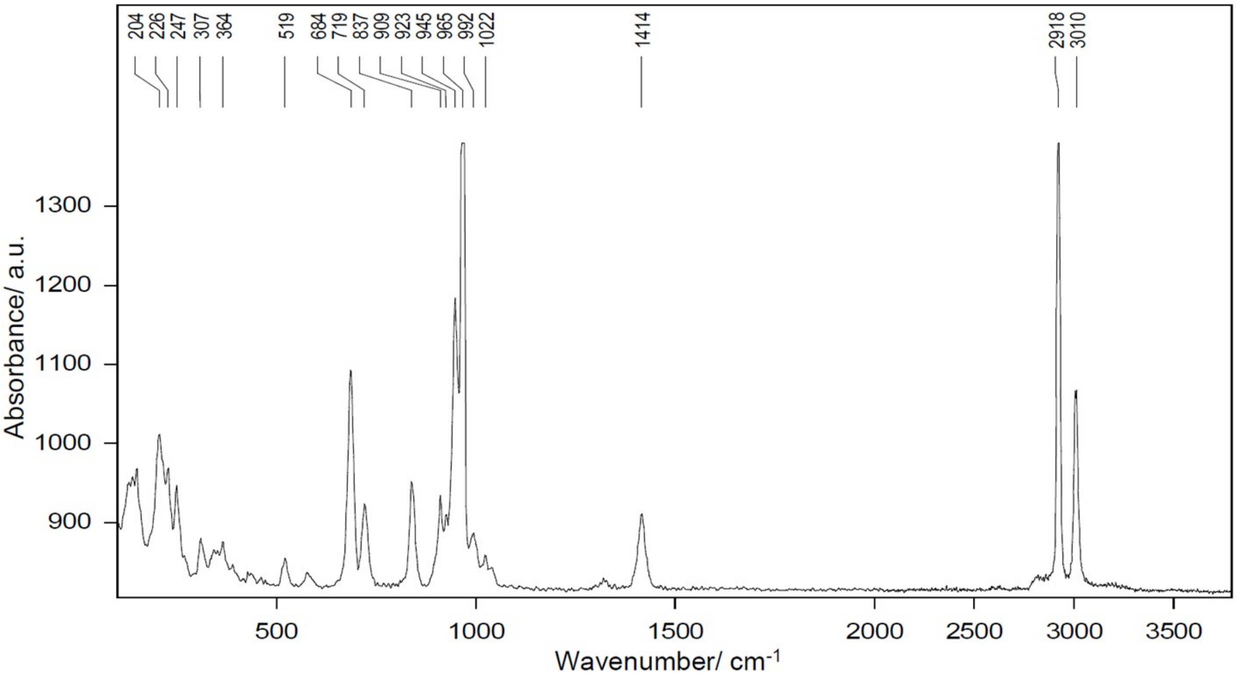

Figure S21: Raman spectrum of compound $(NH_4)[Bi(DMSO)_7][Mo_8O_{26}]\cdot H_2O$ (**2**$\cdot H_2O$)

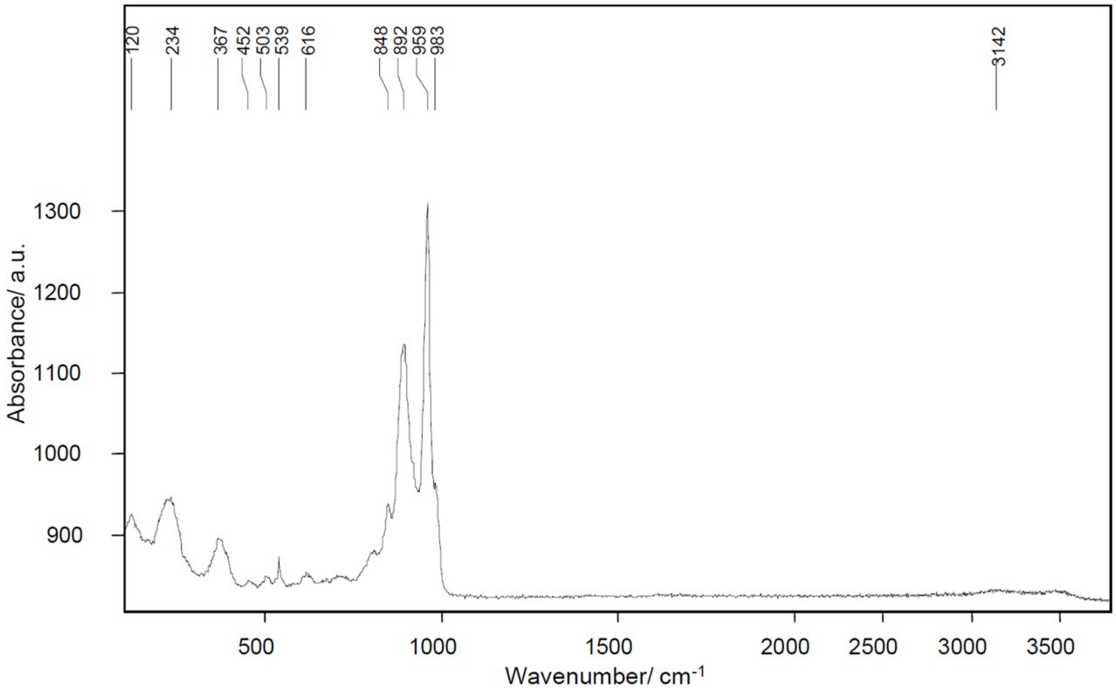

Figure S22: Raman spectrum of compound $[(NH_4)_4(Mo_{36}O_{108}(OH)_4\cdot16H_2O)]\cdot45H_2O$ (**3**$\cdot45H_2O$)

TGA Analysis

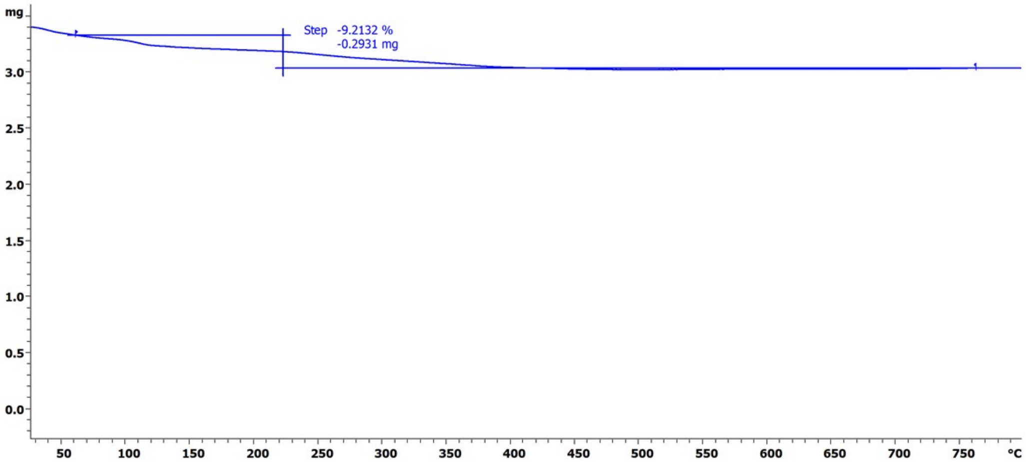

Figure S23: TGA plot of Compound $(NH_4)_{14}[Bi_2W_{22}O_{76}]\cdot14H_2O$ (**1**$\cdot14H_2O$). The mass loss around 9.23% can be attributed to the loss of lattice NH_4^+ and H_2O molecules.

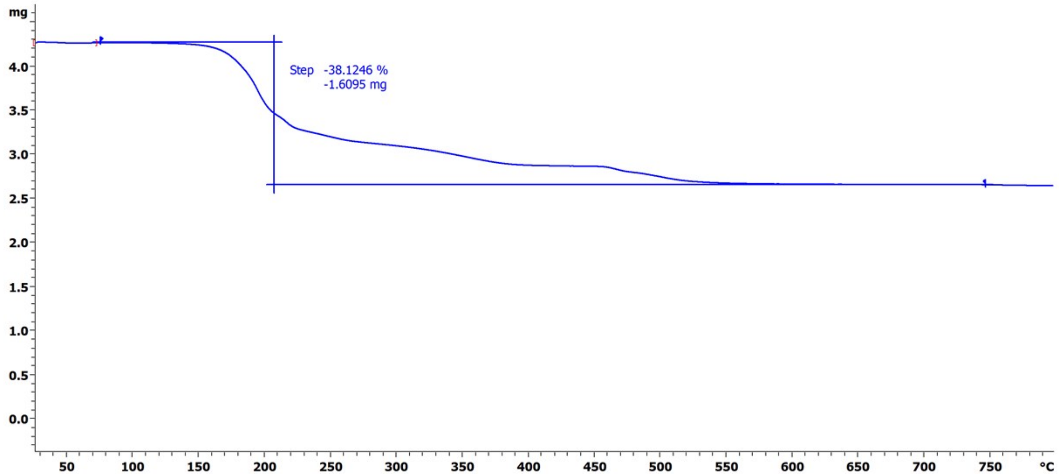

Figure S24: TGA plot of Compound $(NH_4)[Bi(DMSO)_7][Mo_8O_{26}]\cdot H_2O$ (**2**$\cdot H_2O$). The mass loss around 38.12% can be attributed to the loss of H_2O, NH_4^+ and DMSO molecules.

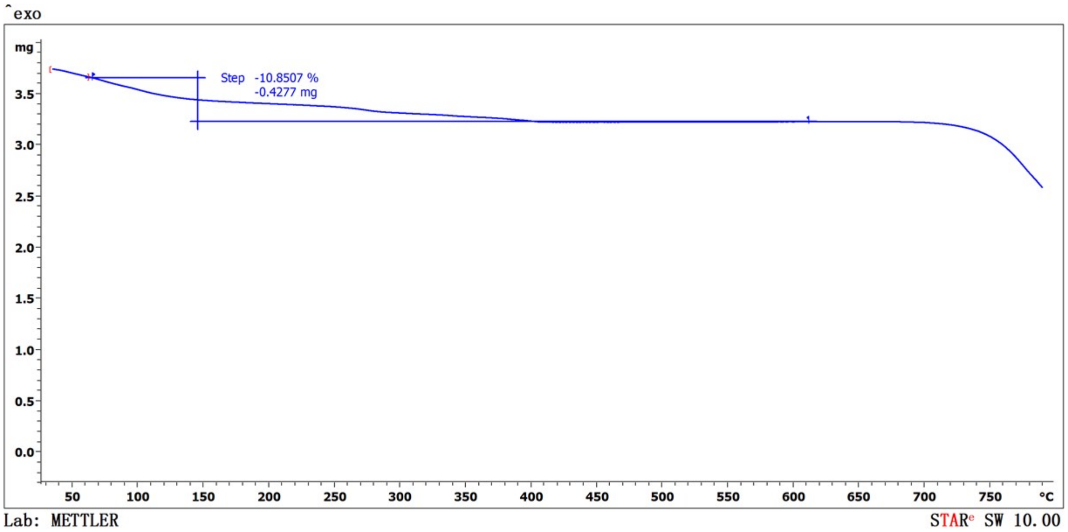

Figure S25: TGA plot of Compound $[(NH_4)_4(Mo_{36}O_{108}(OH)_4\cdot 16H_2O)]\cdot 45H_2O$ (**3**$\cdot 45H_2O$). The mass loss around 10.88% can be attributed to the loss of H_2O and NH_4^+ molecules.

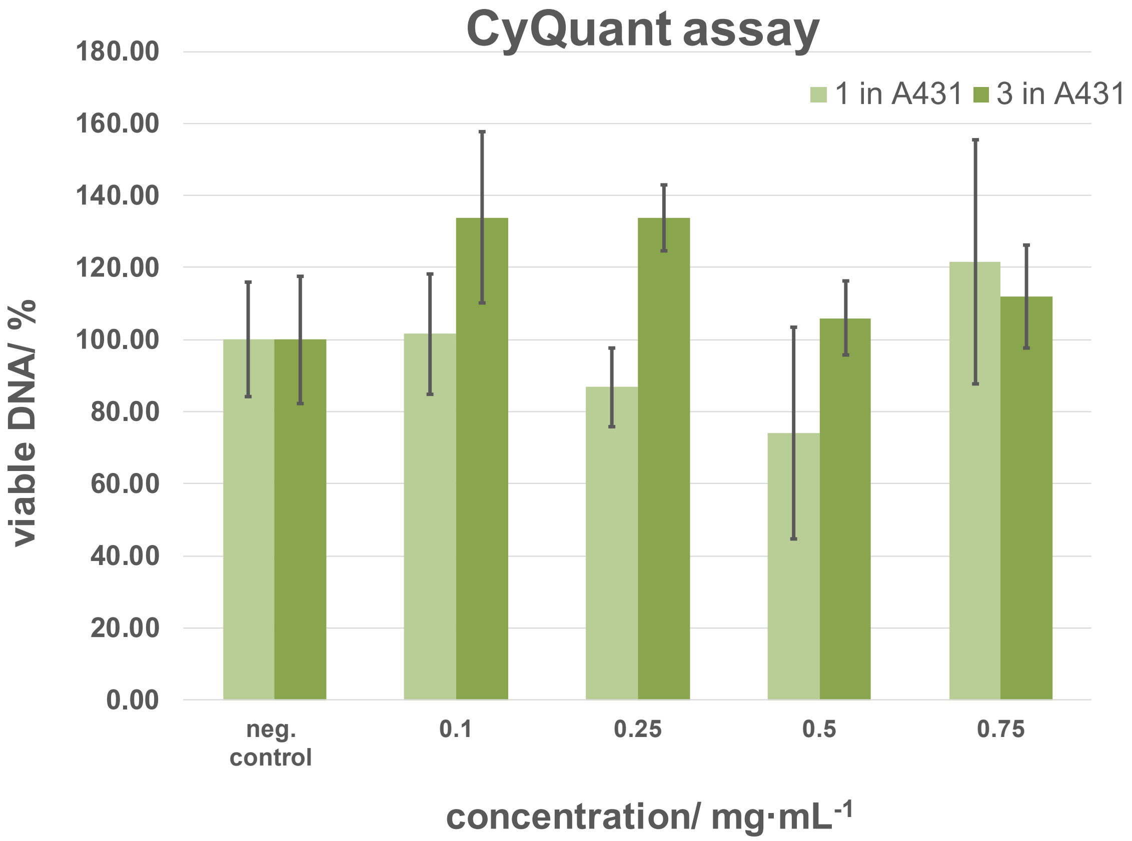

Figure S26: CyQuant assay of **1** and **3** using different concentrations (0, 0.1, 0.25, 0.5 and 0.75 mg/mL) in A431 cell line after 24 h incubation. The percentage of viable DNA is expressed relative to untreated control cells.

References

[1] G. M. Sheldrick, **2002**.

[2] W. Kabsch, *J. Appl. Crystallogr.* **1993**, *26*, 795.

[3] G. M. Sheldrick, *Acta Crystallogr. Sect. A Found. Crystallogr.* **2007**, *64*, 112.

[4] G. M. Sheldrick, *Acta Crystallogr. Sect. C Struct. Chem.* **2015**, *71*, 3.